Some Comments on the Acoustic Coupling of Elements in an Array

K. Watson

May 1990

JSR-89-290

JASON
The MITRE Corporation
7525 Colshire Drive
McLean, Virginia 22102-3481
(703) 883-6997

UNCLASSIFIED

SECURITY CLASSIFICATION OF THIS PAGE

REPORT DOCUMENTATION PAGE

Form Approved OMB No. 0704-0188

1a. REPORT SECURITY CLASSIFICATION UNCLASSIFIED	1b. RESTRICTIVE MARKINGS None
2a. SECURITY CLASSIFICATION AUTHORITY N/A SINCE UNCLASSIFIED	3. DISTRIBUTION / AVAILABILITY OF REPORT Approved for Public Release Distribution Unlimited
2b. DECLASSIFICATION / DOWNGRADING SCHEDULE N/A SINCE UNCLASSIFIED	
4. PERFORMING ORGANIZATION REPORT NUMBER(S) JSR-89-290	5. MONITORING ORGANIZATION REPORT NUMBER(S) JSR-89-290
6a. NAME OF PERFORMING ORGANIZATION The MITRE Corporation JASON Program Office 6b. OFFICE SYMBOL (If applicable) A10	7a. NAME OF MONITORING ORGANIZATION DARPA
6c. ADDRESS (City, State, and ZIP Code) 7525 Colshire Drive McLean, VA 22102	7b. ADDRESS (City, State, and ZIP Code) Defense Advanced Research Project Agency 1400 Wilson Boulevard Arlington, VA 22209-2308
8a. NAME OF FUNDING / SPONSORING ORGANIZATION DARPA 8b. OFFICE SYMBOL (If applicable)	9. PROCUREMENT INSTRUMENT IDENTIFICATION NUMBER
8c. ADDRESS (City, State, and ZIP Code) Defense Advanced Research Project Agency Arlington, VA 22209-2308	10. SOURCE OF FUNDING NUMBERS PROGRAM ELEMENT NO. / PROJECT NO. 8503Z / TASK NO. / WORK UNIT ACCESSION NO.
11. TITLE (Include Security Classification) Some Comments on the Acoustic Coupling of Elements in An Array	
12. PERSONAL AUTHOR(S) K. Watson	
13a. TYPE OF REPORT Technical 13b. TIME COVERED FROM _____ TO _____	14. DATE OF REPORT (Year, Month, Day) 15. PAGE COUNT
16. SUPPLEMENTARY NOTATION	
17. COSATI CODES FIELD / GROUP / SUB-GROUP	18. SUBJECT TERMS (Continue on reverse if necessary and identify by block number) radiated power, acoustic coupling within an array,

19. ABSTRACT (Continue on reverse if necessary and identify by block number)

The effects of acoustic coupling between radiators is investigated for linear and planar acoustic arrays. To provide a simple model for calculation and inversion of the acoustic impedance matrices, spherical radiators are chosen. Considerations of total radiated beam power are addressed. The principal effect of element interaction on array performance found is in the effective impedance of individual radiators in the array.

20 DISTRIBUTION / AVAILABILITY OF ABSTRACT ☐ UNCLASSIFIED/UNLIMITED ☐ SAME AS RPT. ☐ DTIC USERS	21 ABSTRACT SECURITY CLASSIFICATION UNCLASSIFIED
22a. NAME OF RESPONSIBLE INDIVIDUAL Dr. Robert G. Henderson	22b. TELEPHONE (Include Area Code) (703) 883-6997 22c. OFFICE SYMBOL JASON Program Office

DD Form 1473, JUN 86 Previous editions are obsolete. SECURITY CLASSIFICATION OF THIS PAGE

UNCLASSIFIED

Abstract

The effects of acoustic coupling between radiators is investigated for linear and planar acoustic arrays. To provide a simple model for calculation and inversion of the acoustic impedance matrices, spherical radiators are chosen. Considerations of total radiated beam power are addressed. The principal effect of element interaction on array performance found is in the effective impedance of individual radiators in the array.

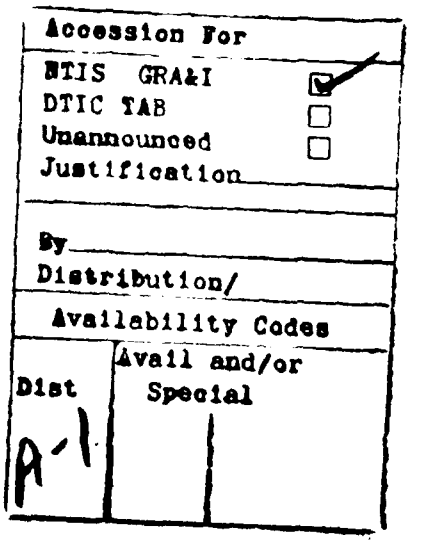

Contents

1 INTRODUCTION

In this note we address some questions related to acoustic coupling between transmitting elements in an acoustic array. We shall be primarily concerned with elements of characteristic size a that are small compared with the acoustic wavelength λ:

$$a \ll \lambda. \tag{1-1}$$

We shall also suppose that the array is operated in a linear acoustic regime. This will be interpreted as implying that the acoustic pressure $p(a)$ at the transducer is less than p_{cav}, that at which cavitation occurs:

$$p(a) \ll p_{\mathrm{cav}}. \tag{1-2}$$

The array is assumed to have N_r radiators with phase centers at locations $\mathbf{x}_i (i = 1, \ldots N_r)$ in the neighborhood of the origin of a rectangular coordinate system. Taking advantage of condition Equation (1-1) we compromise slightly on generality by assuming spherical radiators of radius a that are driven in a spherically symmetric mode. Then the acoustic pressure at a distance R_i from the ith element is

$$p_i(\mathbf{r}) = p_i(a)(a/R_i)e^{ik(R_i - a)}, \tag{1-3}$$

where

$$\mathbf{R}_i = \mathbf{r} - \mathbf{x}_i.$$

Since we have assumed a linear system, the total acoustic pressure at $\mathbf{r}$ is

$$p(\mathbf{r}) = \sum_{i=1}^{N_r} p_i(\tilde{r}). \tag{1-4}$$

In the far field of the array we can write this as

$$p(\mathbf{r}) \cong p_o(a/R)e^{ikR}D(\hat{\mathbf{r}}), \tag{1-5}$$

where, to within an unimportant phase factor,

$$D(\hat{\mathbf{r}}) \equiv \sum_{i=1}^{N_r} (p_i(a)/p_o)e^{ik\hat{\mathbf{r}}\cdot\mathbf{x}_i} \tag{1-6}$$

and, say,

$$p_o = \sum_i |p_i(a)|\, N_r. \qquad (1-7)$$

The maximum radiated beam power will occur in a given direction $\mathbf{r}$ when the phases of the $p_i(a)$ are adjusted so that

$$D(\mathbf{r}) = N_r.$$

In this case the maximum radiated power/unit solid angle is

$$\begin{aligned} P_{\text{beam}} &= r^2|p|^2/(2\rho c) \qquad (1\text{-}8) \\ &= \frac{a^2 p_o^2}{2\rho c} N_R^2. \end{aligned}$$

[Here $\rho \approx 1000$ kg/m^3 and $c \approx 1500$ m/s is the speed of sound.]

The total radiated power is

$$P_{\text{rad}} = \int \frac{|p(\mathbf{r})|^2}{2\rho c} r^2 d\Omega, \qquad (1-9)$$

where the integral is over all solid angles Ω . We obtain

$$\begin{aligned} P_{\text{rad}} &= \frac{4\pi a^2}{2\rho c} \left\{ \sum_{i=1}^{N_r} |p_i(a)|^2 \right. \qquad (1\text{-}10) \\ &+ \left. \sum p_i^*(a) p_j(a) \frac{\sin[k|\mathbf{x}_i - \mathbf{x}_j|]}{k|\mathbf{x}_i - \mathbf{x}_j|} \right\}. \end{aligned}$$

Of special interest is a linear or planar array for which the radiated beam is "broadside," or $\mathbf{r} \cdot \mathbf{x}_i = 0$. Then, if maximum beam power is desired the driving phases will be equal, so

$$\begin{aligned} P_{\text{rad}} &= \frac{4\pi a^2}{2\rho c} \left\{ \sum_{i=1}^{N_r} |p_i(a)|^2 \right. \qquad (1\text{-}11) \\ &+ \left. \sum_{i \neq j} |p_i(a)|\, |p_j(a)| \frac{\sin[k|\mathbf{x}_i - \mathbf{x}_j|]}{k|\mathbf{x}_i - \mathbf{x}_j|} \right\}. \end{aligned}$$

When high beam power is the objective, the second term in Equation (1-10) is not of great significance (see Section 2) and we have

$$\begin{aligned} P_{\text{rad}} &\cong \frac{4\pi a^2}{2\rho c} \sum_i |p_i(a)|^2 \qquad (1\text{-}12) \\ &\leq 4\pi a^2 N_r \left(\frac{p_{\text{cav}}^2}{2\rho c} \right). \end{aligned}$$

For purposes of illustration, we shall take

$$p_{\text{cav}}^2/(2\rho c) = 13KW/m^2, \qquad (1-13)$$

so

$$P_{\text{rad}} \leq 4\pi a^2 N_r x[13KW/m^2]. \qquad (1-14)$$

Returning to Equation (1-8), we conclude that

$$P_{\text{beam}} \leq a^2 N_r^2 x[13KW/m^2]. \qquad (1-15)$$

The bounds in Equations (1-12) and (1-15) on the total radiated power [see the clarification in Section 2] and on the beam power/steradian appear to be fundamental for simple arrays operating in a linear regime. The quadratic dependence on element radius indicates the price which is paid in total radiated energy in exchange for the price saved with small radiators.

Our argument does not bound radiators working in a nonlinear regime or radiators placed near reflectors, baffles, etc.

In Section 2 we examine the role of the second term in Equations (1-10) and (1-11). In Section 3 we investigate the performance of an array when close acoustic coupling between radiating elements obtains.

2 THE TOTAL RADIATED POWER

In this Section we consider the effect of element displacement in changing the total radiated power in an array. For a linear or planar array with broadside steering we can replace Equation (1-11) by

$$P' = 1 + \frac{1}{N_r} \sum_{i \neq j} \frac{\sin[k|\mathbf{x}_i - \mathbf{x}_j|]}{k|\mathbf{x}_i - \mathbf{x}_j|}, \qquad (2-1)$$

dropping multiplicative factors.

First we consider a linear array with $\lambda/2$ element spacing. Then $P' = 1$. Evidently, we can maximize Equation (2-1) by setting all the $\mathbf{x}_i$ equal. Then $P' = N_r$, but we have no beam forming! Various more restrictive algorithms have been tried, none of which increase beam power [consistent with Equation (1-8)]. We illustrate this for a 10 element array and a simple algorithm that holds fixed the first and last elements at positions 0 and 4.5 (we shall scale all lengths in units of $\lambda/2$). The remaining 8 elements are sequentially moved between neighbors to maximize P', but constrained so no two elements can be closer than 1/8. Starting with an element spacing of 1/2 and $P' = 1$, the algorithm converged in a few iterations to the spacing shown in Figure 1 and

$$P' = 2.57. \qquad (2-2)$$

The resulting beam pattern is shown in Figure 2. The extra radiated energy is fed into sidelobes, as might have been anticipated from Equation (1-8).

As a second example we consider a square array of 5 rows, each having 5 elements. The spacing of rows and elements is 1/2 (i.e. $\lambda/2$). For this 25 element array,

$$P' = 1.01. \qquad (2-3)$$

With sequential moving of elements between neighbors and rows between rows (holding boundaries fixed and permitting no elements or rows to be closer than 1/8) we are led to the element positions shown in Figure 3 and

$$P' = 4.45. \qquad (2-4)$$

Again, this extra radiated energy has gone into sidelobes rather than beam power.

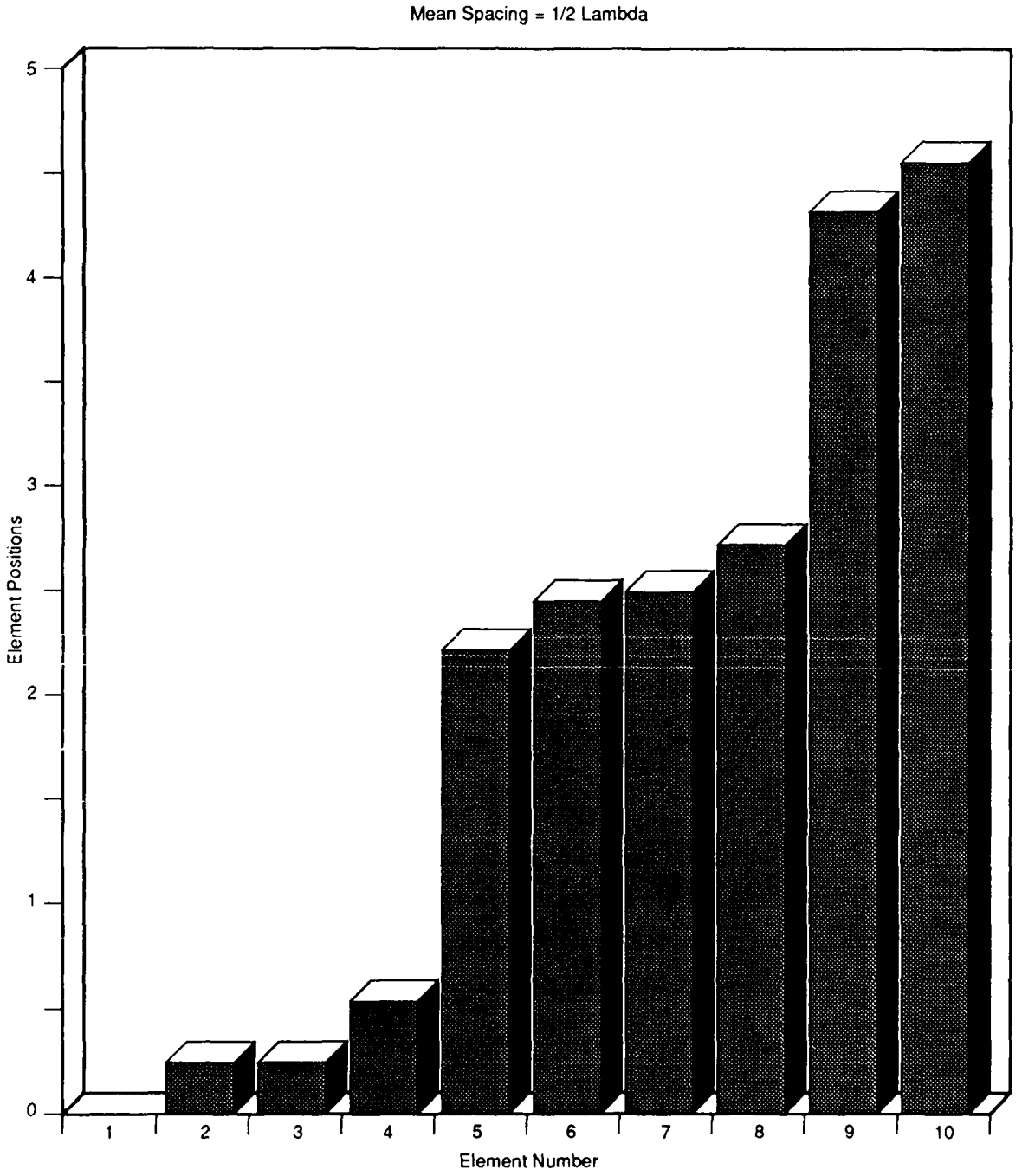

Figure 1 Element spacing for a 10 element linear array to maximize the radiated power (2.1).

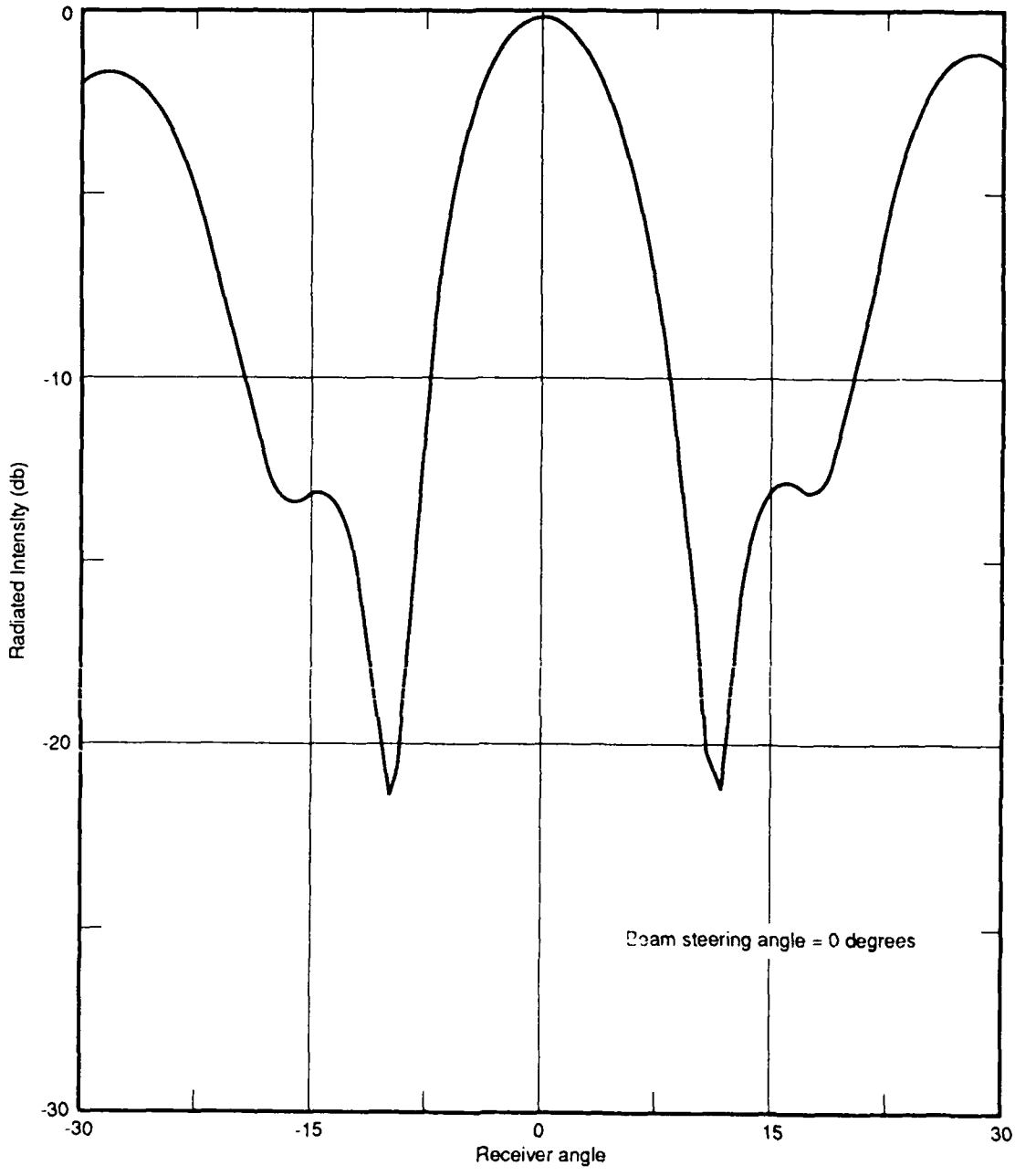

Figure 2 Beam pattern for the array shown in Figure (1).

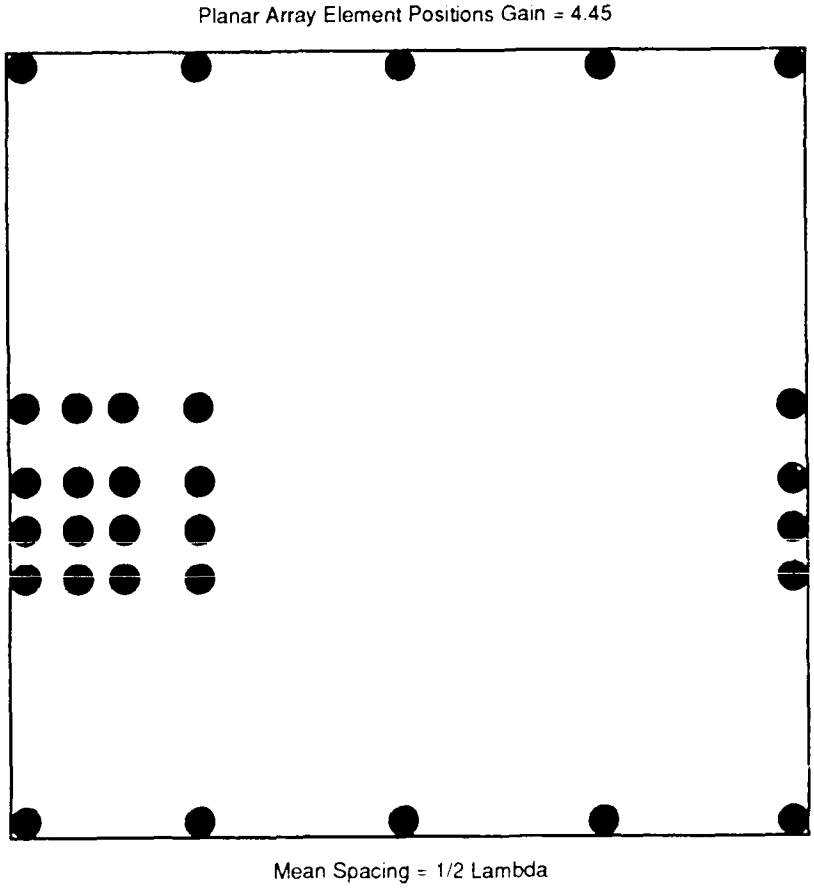

Figure 3 Element spacing to maximize (2.1) for a 25 element square array.

3 ACOUSTIC COUPLING WITHIN AN ARRAY

In this Section we look in some detail at the beam forming mechanism for our simple model of N_r identical spherical radiators in a linear or planar array. The radius of a radiator is $a + \zeta$, where

$$\dot{\zeta} = w, \text{ the surface velocity} \qquad (3-1)$$

and

$$|\zeta| \ll a.$$

We also assume simple harmonic radiation:

$$w = V\, e^{i\omega t}. \qquad (3-2)$$

Then the acoustic pressure at the radiator surface is

$$p(a) = Zw \qquad (3-3)$$

where

$$Z = \rho\, cka/(ka + i) \qquad (3-4)$$

is the acoustic impedance. In obtaining Equation (3-3) we have used the relation

$$\partial p/\partial r = i\omega\rho w$$

and Equation (1-3).

For the array of N_r elements the average pressure at the surface of element i is

$$p_i(a) = \sum_{j=1}^{N_r} Z_{ij} w_j \qquad (3-5)$$

where

$$w_j = V_j\, e^{-i\omega t}. \qquad (3-6)$$

The average pressure in Equation (3-5) is defined as

$$p_i(a) = \int \frac{p(\mathbf{r})}{1\pi a^2} dS \qquad (3-7)$$

where the integration extends over the spherical element surface. Using Equations (1-3),(3-3), and (3-7) we obtain

$$Z_{ij} = Z\frac{a}{R_{ij}}e^{ik(R_{ij}-a)}\frac{\sin(ka)}{ka}. \qquad (3-8)$$

We note at this point that the relation Equation (3-5) neglects scattering of radiation by the radiators. This scattering is dependent on the specific array geometry and is expected to be small for small radiators. For the sphere i and radiation from j we have [see M. Junger and D. Feit, Sound, Structures and Their Interactions. MIT Press, 1986]

$$\frac{p_{\text{scattered}}}{p_{\text{radiated}}} \approx (ka)^2(a/R_{ij}). \qquad (3-9)$$

At any rate, we shall neglect sound scattering within the array.

The equations for driving the array surface are assumed to have the form

$$M\dot{w}_i + \alpha\, w_i = F_i - p_i(a). \qquad (3-10)$$

Here M is a mass and α is a damping constant characterizing the radiators, and

$$F_i = f_i\, e^{-i\omega t}.$$

On substituting Equation (3-5) into Equation (3-10) and removing the time dependent factors, we obtain

$$[-i\omega\, M + \alpha + Z]V_i = f_i - \sum_{j(\neq i)} Z_{ij}V_j. \qquad (3-11)$$

Now, the $Im(Z)$ represents a mass of water and the $Re(z)$ radiation damping, so we may write

$$\begin{aligned} -Im(Z) &\equiv M_w = \frac{4\pi a^3\rho}{(ka)^2+1} \qquad (3\text{-}12)\\ Re(Z) &= \omega(ka)M_w. \end{aligned}$$

Thus, we can re-write Equation (3-11) as

$$[-i\omega M_r + \alpha_r]V_i = f_i - \sum Z_{ij}V_j. \qquad (3-13)$$

Here

$$\begin{aligned} M_e &= M + M_w \\ \alpha_e &= \alpha + \omega(ka)M_w \\ &= \omega[\frac{M}{4\pi Q} + (ka)M_w] \end{aligned} \tag{3-14}$$

and we have introduced the "Q" of the radiator:

$$Q = \frac{M\omega}{4\pi\alpha}. \tag{3-15}$$

The pressure at great distances from the array is

$$p(r) = Z\left(\frac{a}{r}\right)\sum_{i=1}^{N_r}\exp[ik(R_i - a)]V_i. \tag{3-16}$$

It is convenient to write

$$\begin{aligned} f_i &= |f_i|e^{i\alpha_i} \\ V_i &= |V_i|e^{i\epsilon_i}. \end{aligned} \tag{3-17}$$

To steer a beam in the horizontal direction (from broadside) θ_s we set

$$\epsilon_i = kx_i\sin\theta_s. \tag{3-18}$$

The power input to the array is (for $T \ll \omega^{-1}$)

$$\begin{aligned} P_{in} &= \frac{1}{T}\int_0^T \left\{\sum F_i w_i\right\} dt \\ &= \sum_i |V_i||f|\cos(\alpha_i - \epsilon_i)/2 \end{aligned} \tag{3-19}$$

and the total power radiated is

$$P_{\text{rad}} = \frac{\omega M_w(ka)}{2}\sum_{i=1}^{N_r}|V_i|^2. \tag{3-20}$$

The radiated power in the beam/unit solid angle is obtained using Equations (1-5) and (3-16)

$$P_{\text{beam}} = \frac{r^2|p(r)|^2}{2\rho c}. \tag{3-21}$$

For an array for which acoustic coupling can be neglected we use Equation (3-18) and set $|V_i| = V_0$, all i. Then from Equation (3-13) we find

$$f_i = [-i\omega M_e + \alpha_e]V_o\, e^{i\alpha_i}. \qquad (3-22)$$

These driving forces, with the phases defined by Equation (3-18), will be used as "standard" in Equation (3-13) when we are interested in the coupling.

For numerical illustration we shall consider two arrays. The first is an array of 3 rows each having 7 elements in a horizontal line. The second array has 5 rows each having 5 elements in a horizontal line. Half wavelength spacing is assumed in both arrays. We shall further take

$$Q = 0.2, M_W = M, \text{ and } \omega = 628. \qquad (3-23)$$

With Equation (3-22) as the specified driving force, we can solve the coupled equations, Equation (3-13) for the element surface velocities V_i . The far field pressure is finally obtained from Equation (3-16). We emphasize that for all calculations shown here the driving forces are obtained from Equation (3-22) with the phases set by Equation (3-18).

We first consider radiation from the 7×3 element array when the elements are uncoupled [i.e., $Z_{ij} = 0$ for $i \neq j$ in Equation (3-23)]. For broadside steering (i.e. $\theta_s = 0$) the radiated intensity as a function of observation angle θ (in the horizontal plane and measured from θ_s is shown in Figure 4. The intensity as shown is

$$I(\theta) = 10\log(|D|^2/N_r^2), \qquad (3-24)$$

where D is given by (1-6). In Figures 5 through 8 we show the radiated intensity obtained from coupled elements using Equation (3-13). These are shown for different radiator scaled sizes:

$$\text{dia} = 4a/\lambda. \qquad (3-25)$$

In Figures 9 and 10 we show the radiated intensity for $\theta_s = 30°$.

In the next series of figures, we show the corresponding radiated power from the 5×5 array.

In looking at these figures, we note that increasing the coupling strength (i.e., the element radius a) reduces the effective acoustic impedance and

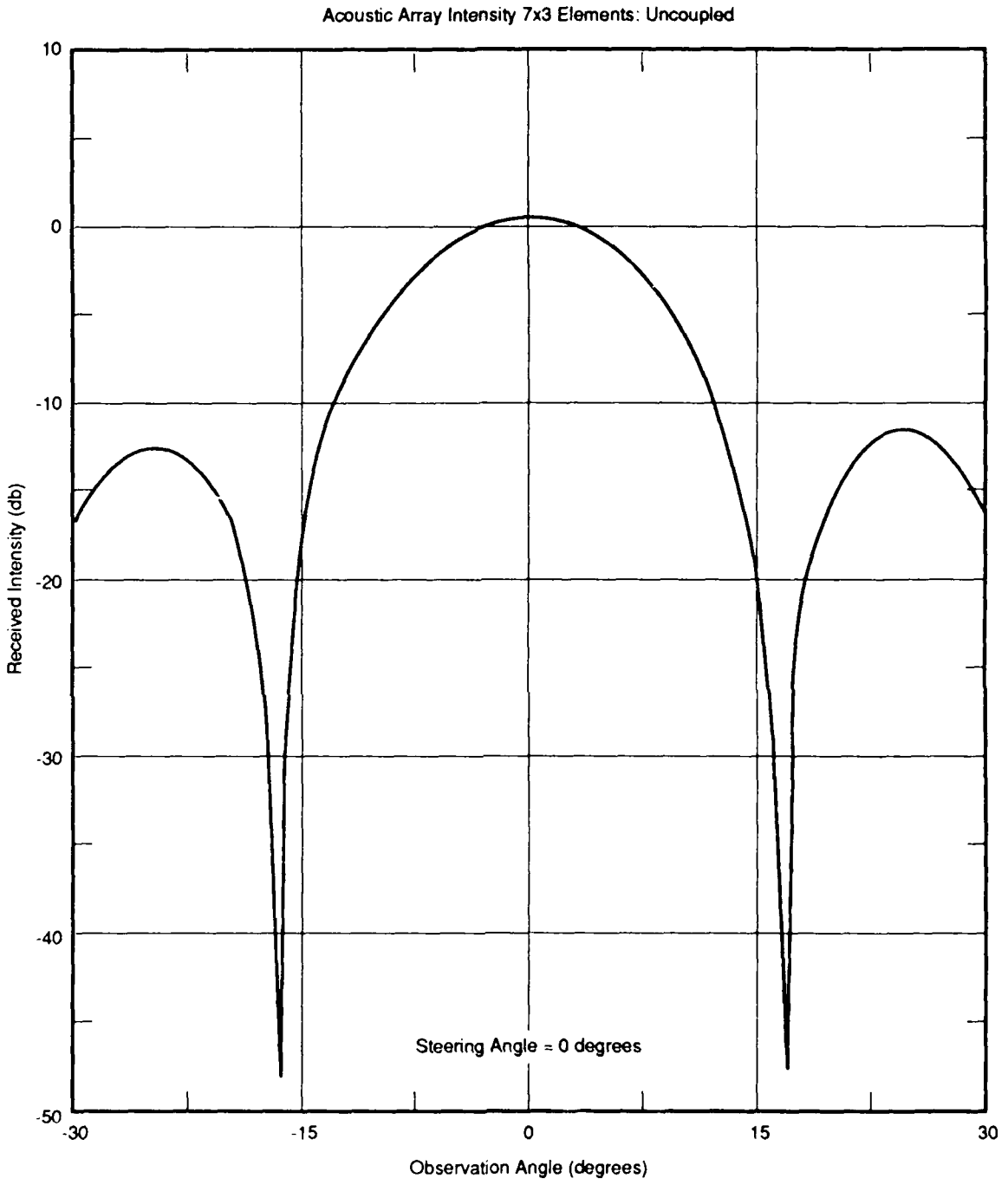

Figure 4 The radiated power (3.24) for the 7x3 array as a function of horizontal angle when the steering angle $\theta_s = 0$.

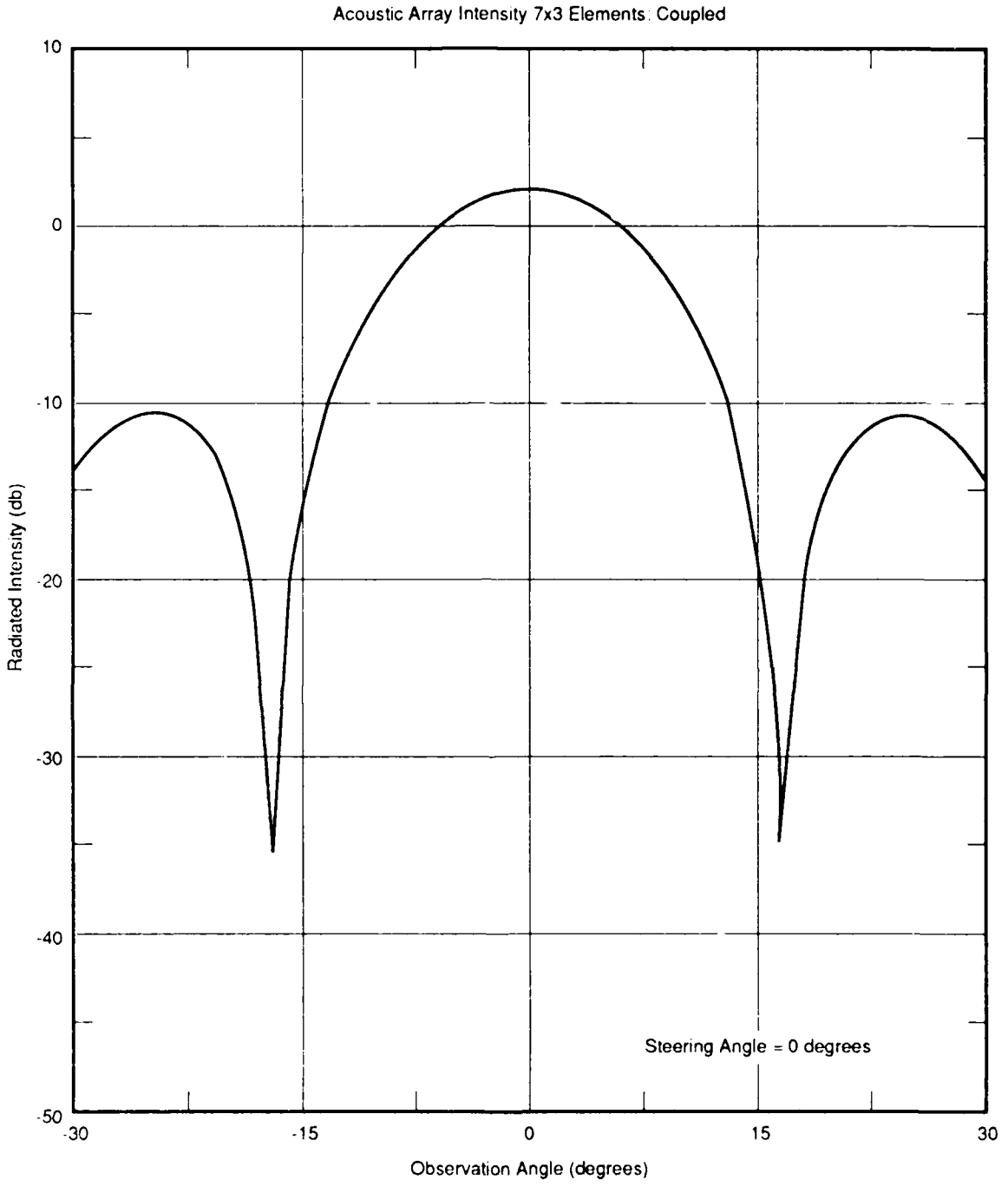

Figure 5 The 7x3 array radiated power for coupled elements, θ_s=0, and an element diameter of 0.38.

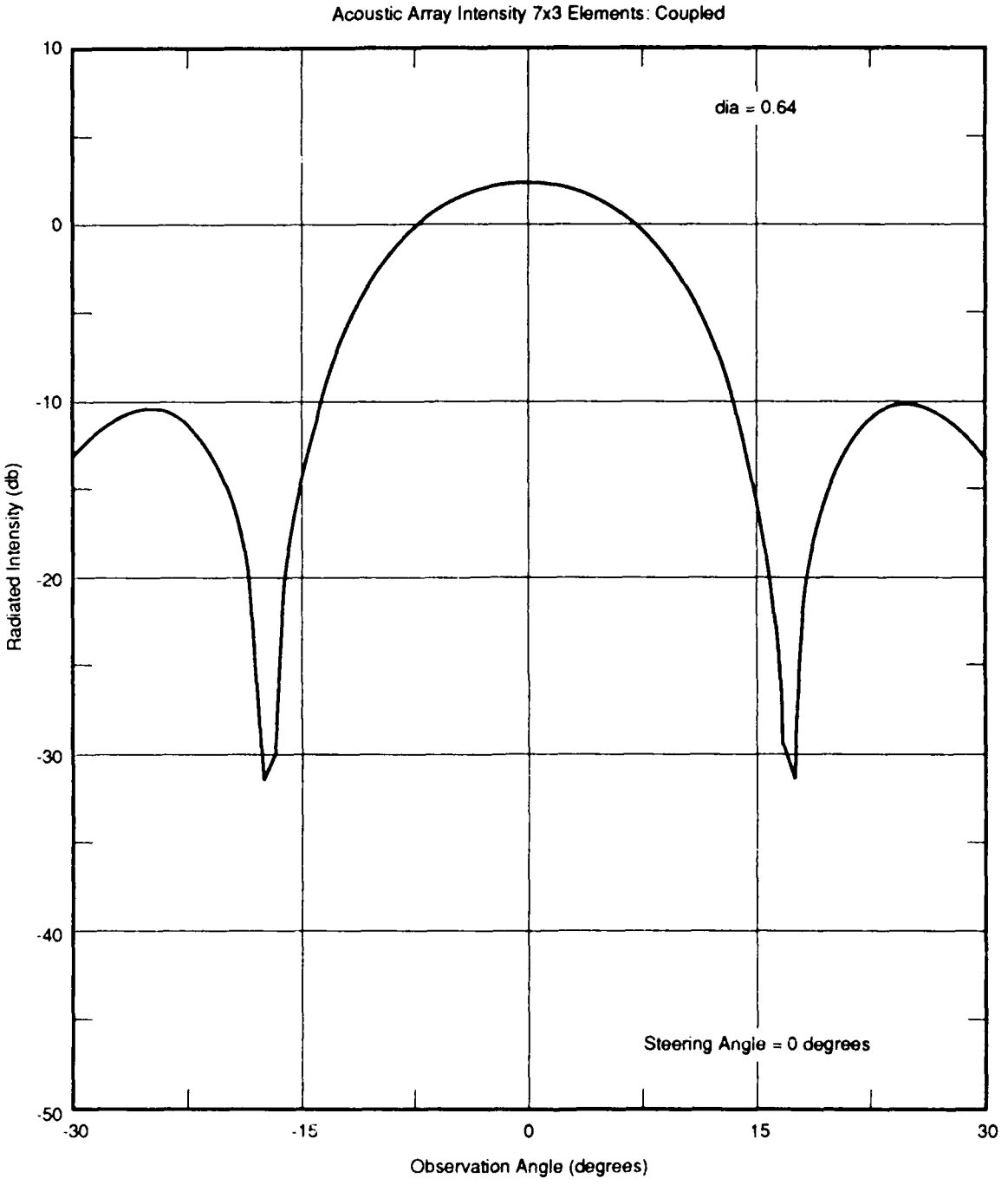

Figure 6 The radiated power, as in Figure (5), but for an element diameter 0.64.

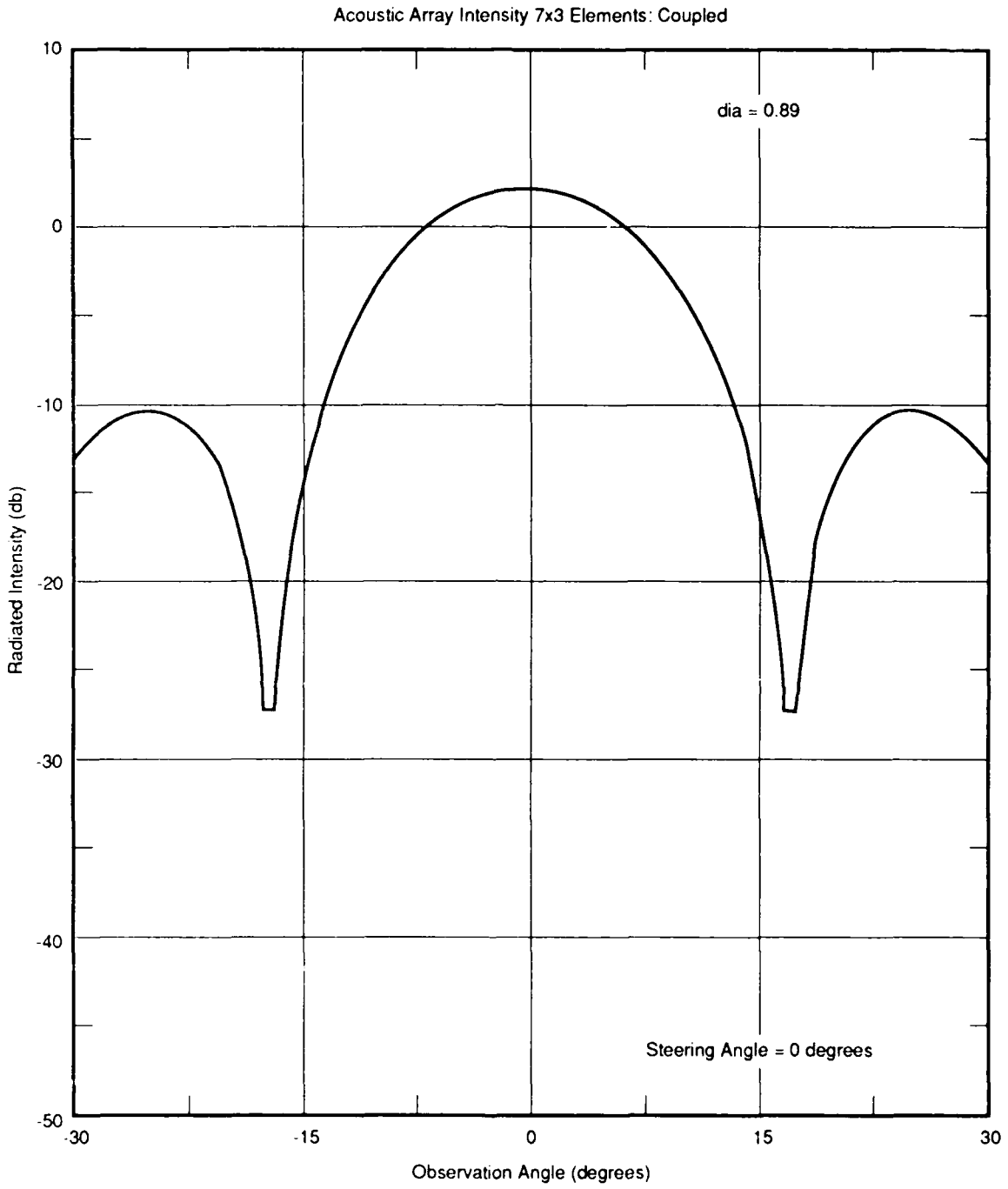

Figure 7 The radiated power, as in Figure (5), but for an element diameter 0.89.

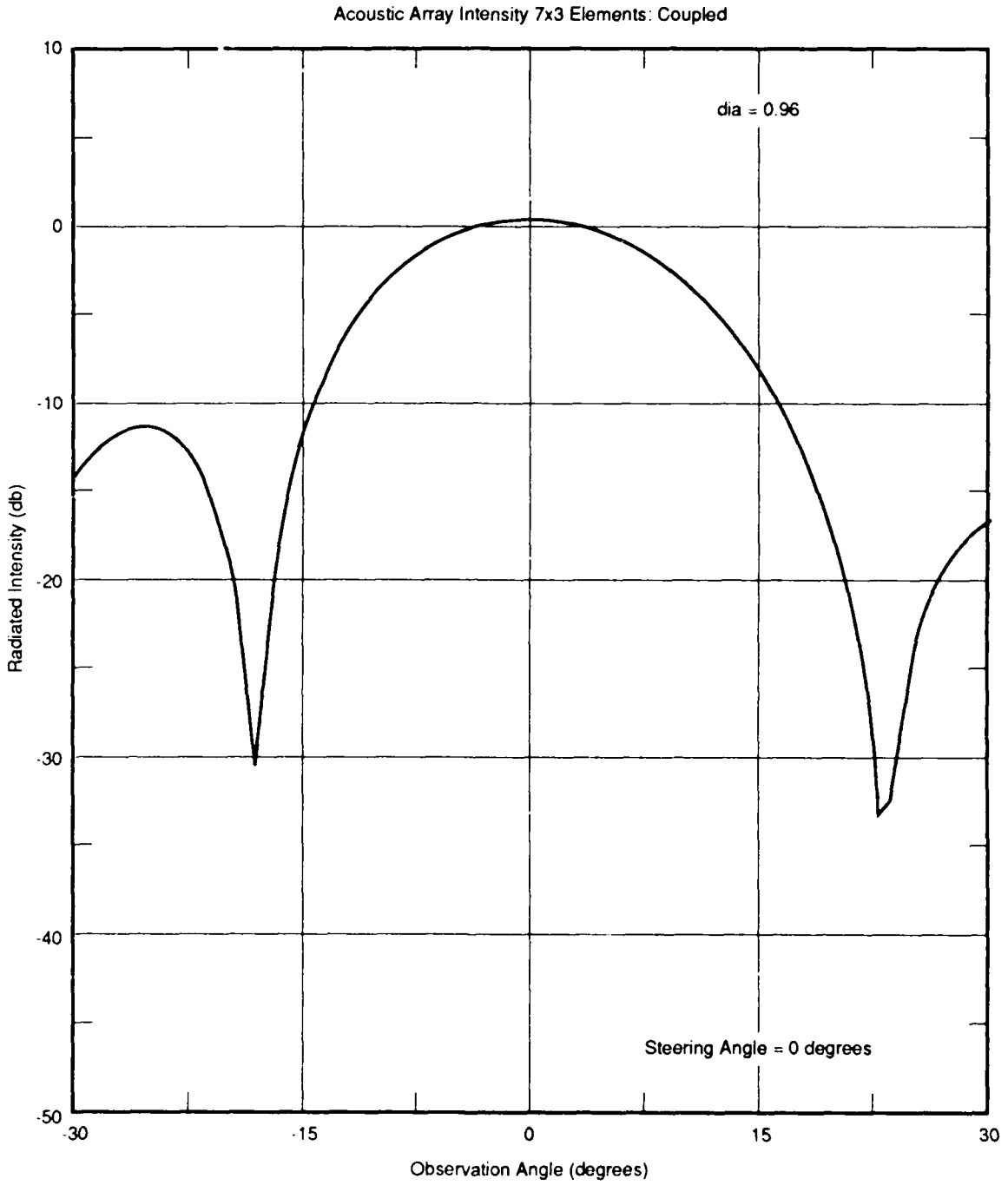

Figure 8 The radiated power, as in Figure (5), but for an element diameter 0.96.

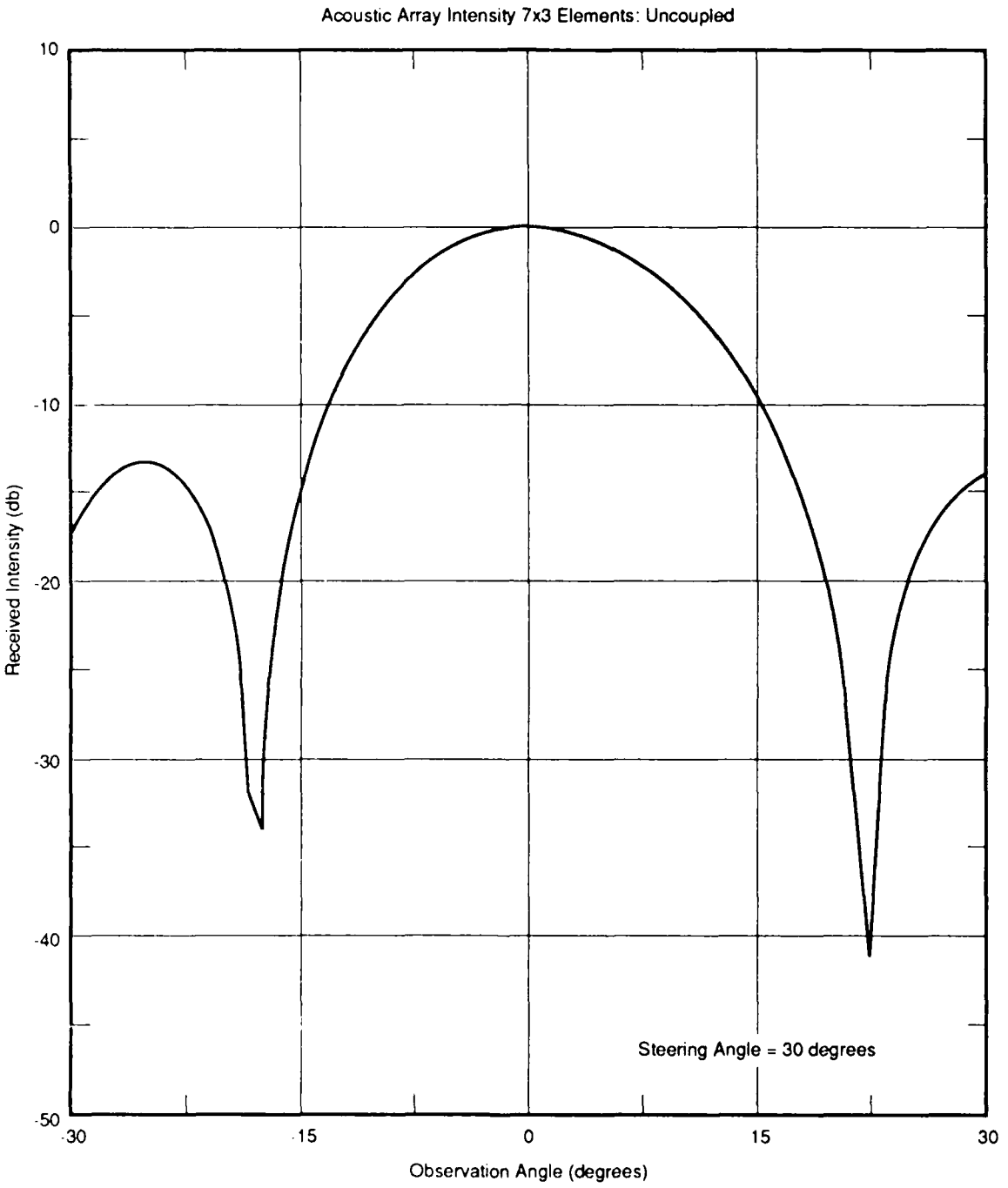

Figure 9 The radiated power, as in Figure (4), but for $\theta_S = 30^\circ$.

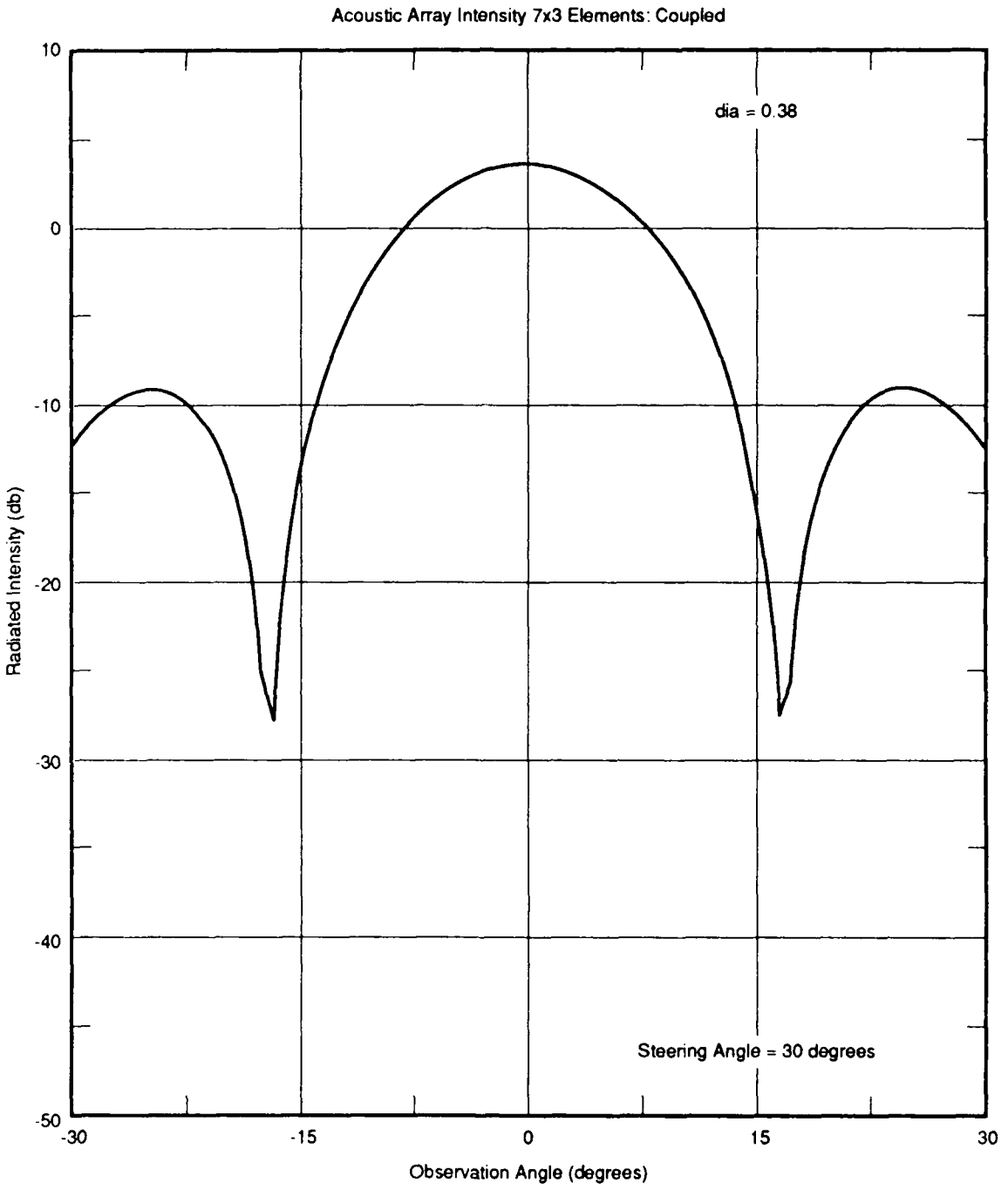

Figure 10 The radiated power, as in Figure (5), but for $\theta_S = 30^{\circ}$.

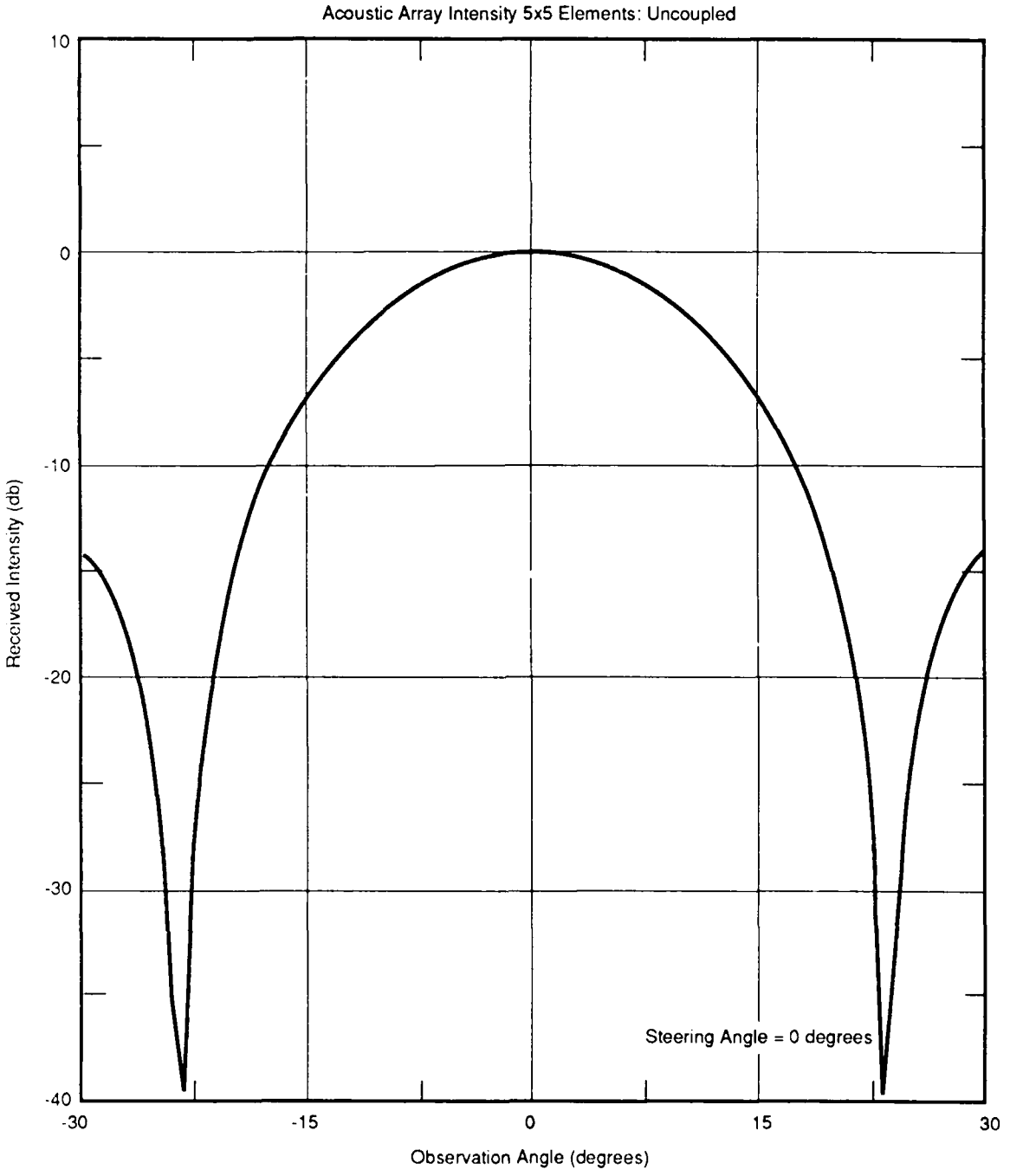

Figure 11 The radiated power (3.24) for the 5x5 array as a function of horizontal angle when the steering angle $\theta_S=0$ and the elements are uncoupled.

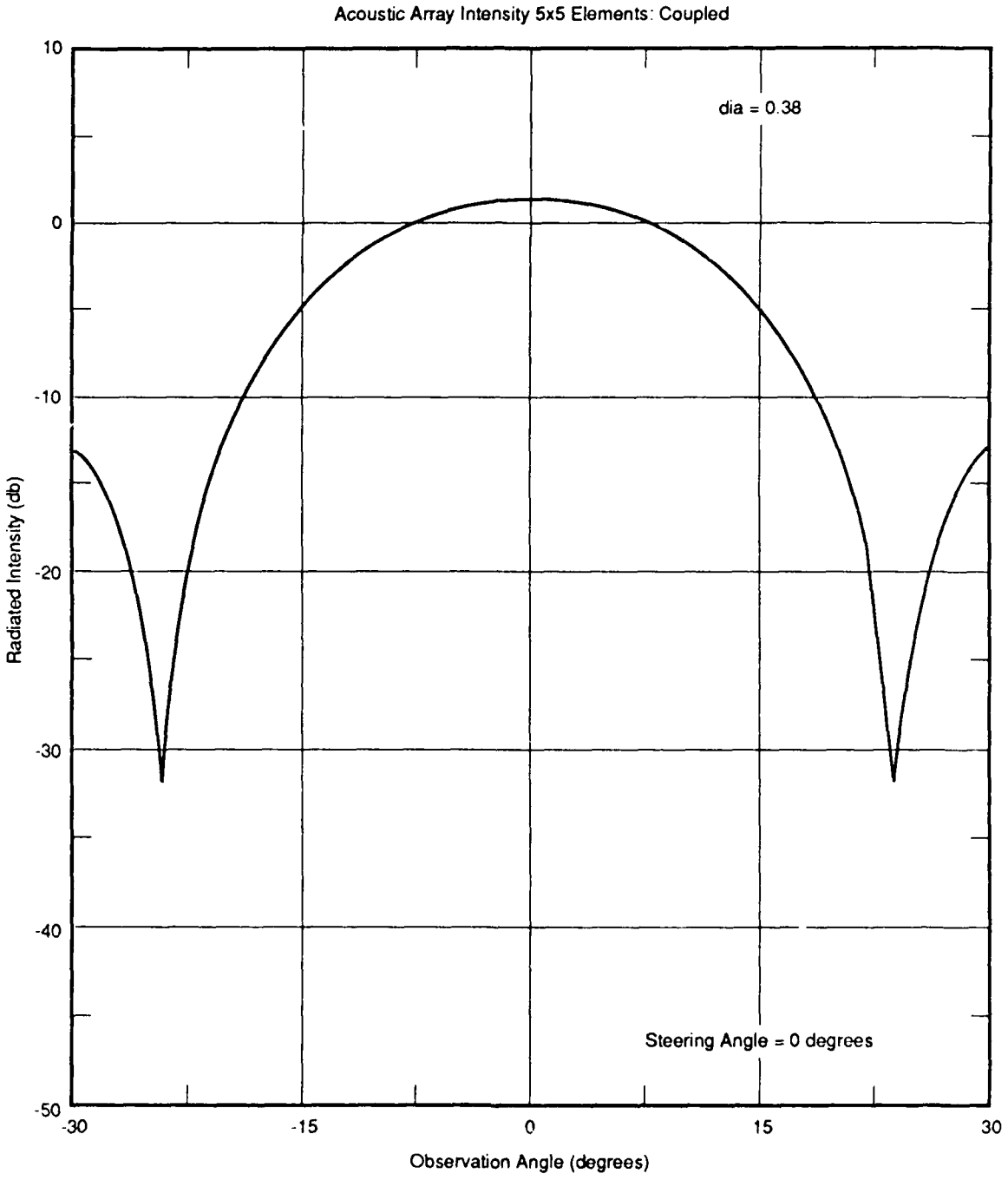

Figure 12 The 5x5 array radiated power for coupled elements, θ_S=0, and an element diameter of 0.38.

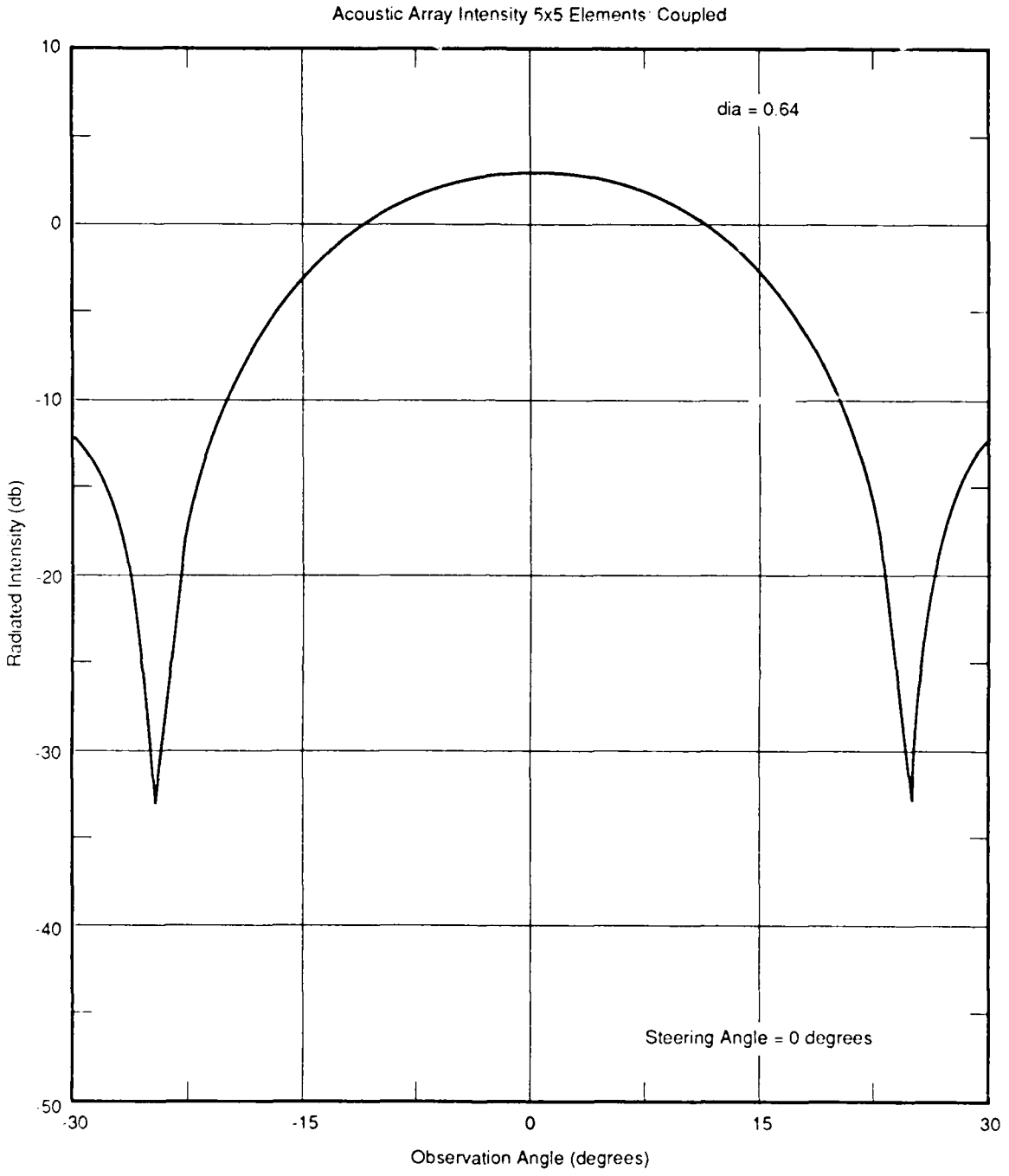

Figure 13 The radiated power, as in Figure (12), but for an element diameter 0.64.

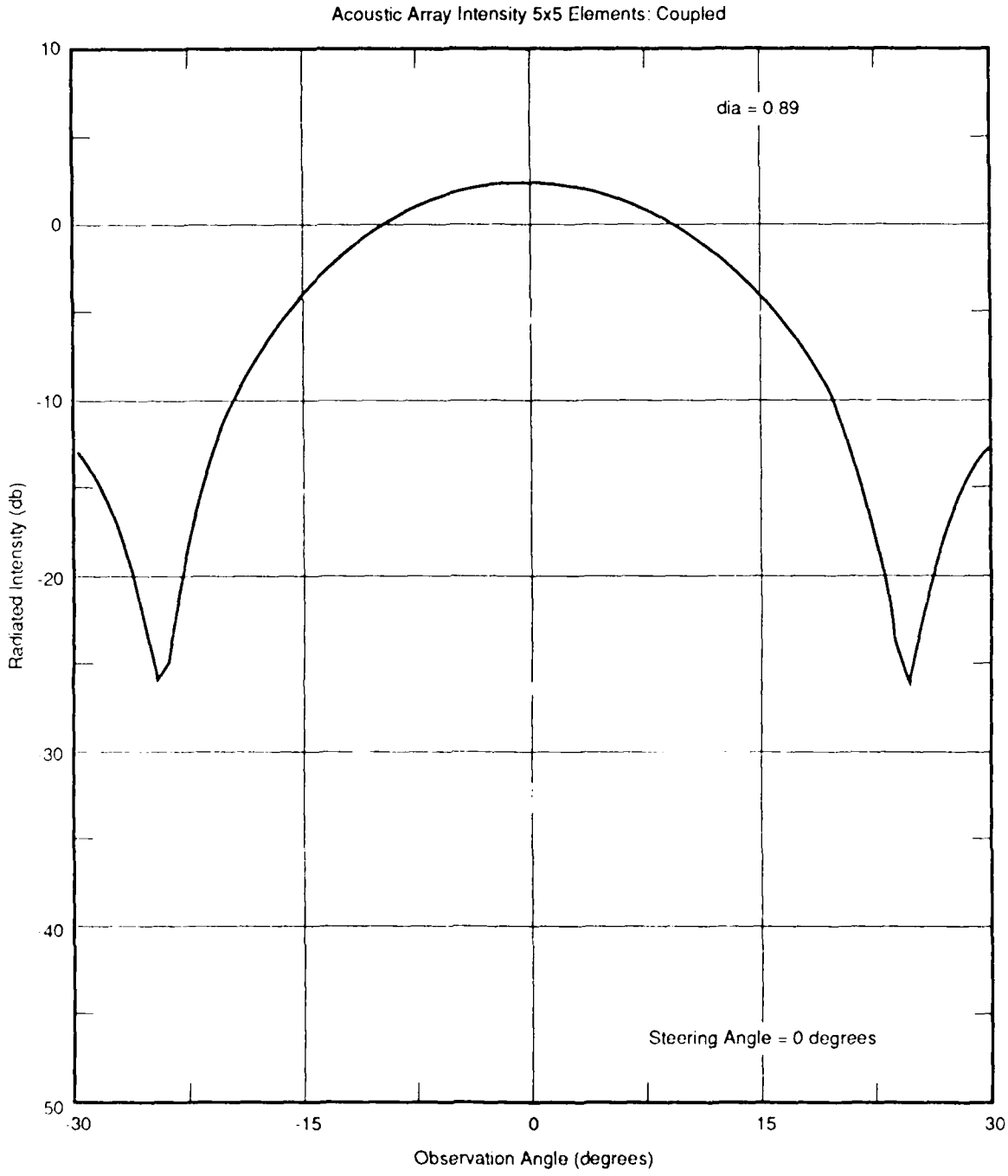

Figure 14 The radiated power, as in Figure (12), but for an element diameter 0.89.

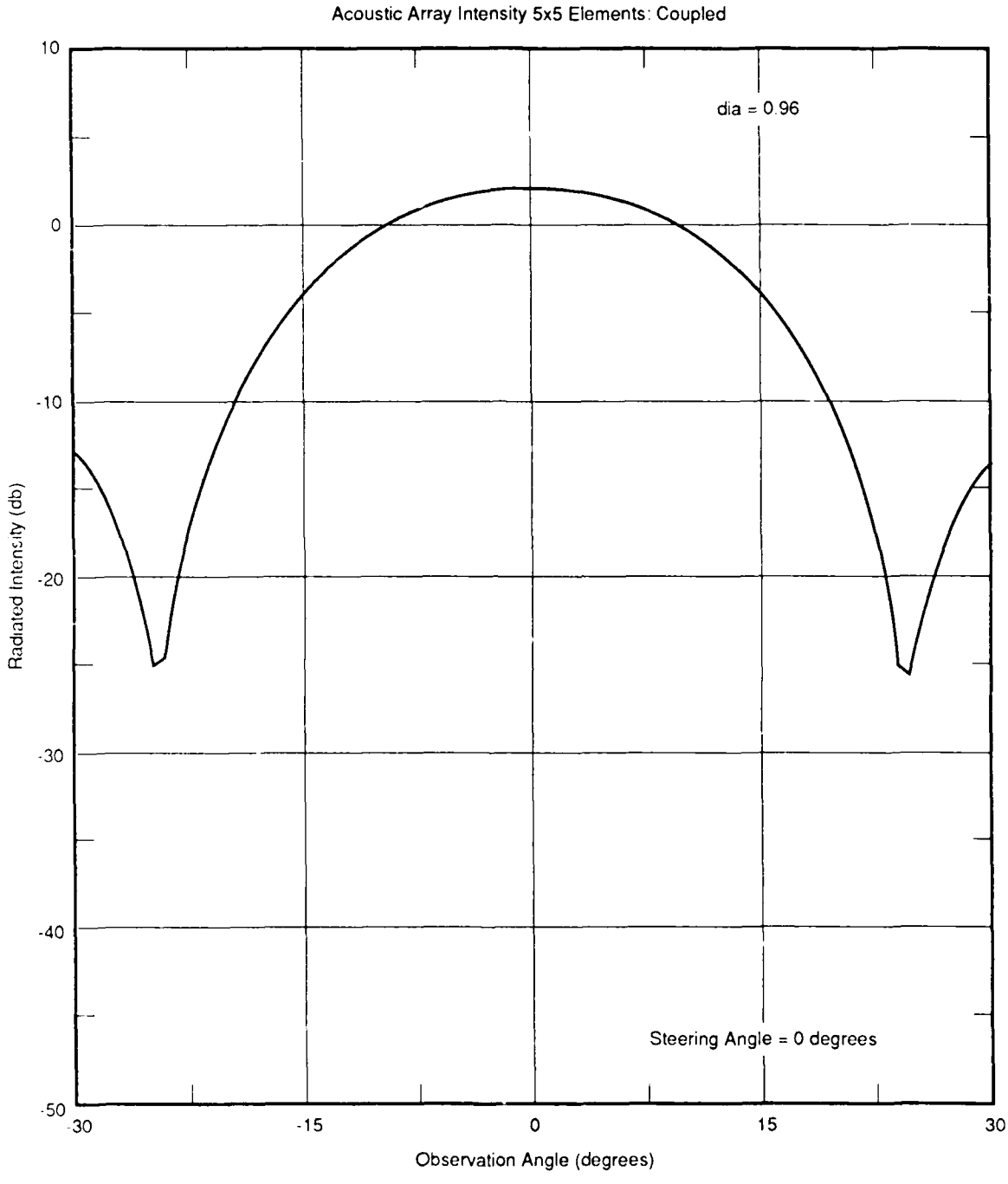

Figure 15 The radiated power, as in Figure (12), but for an element diameter 0.96.

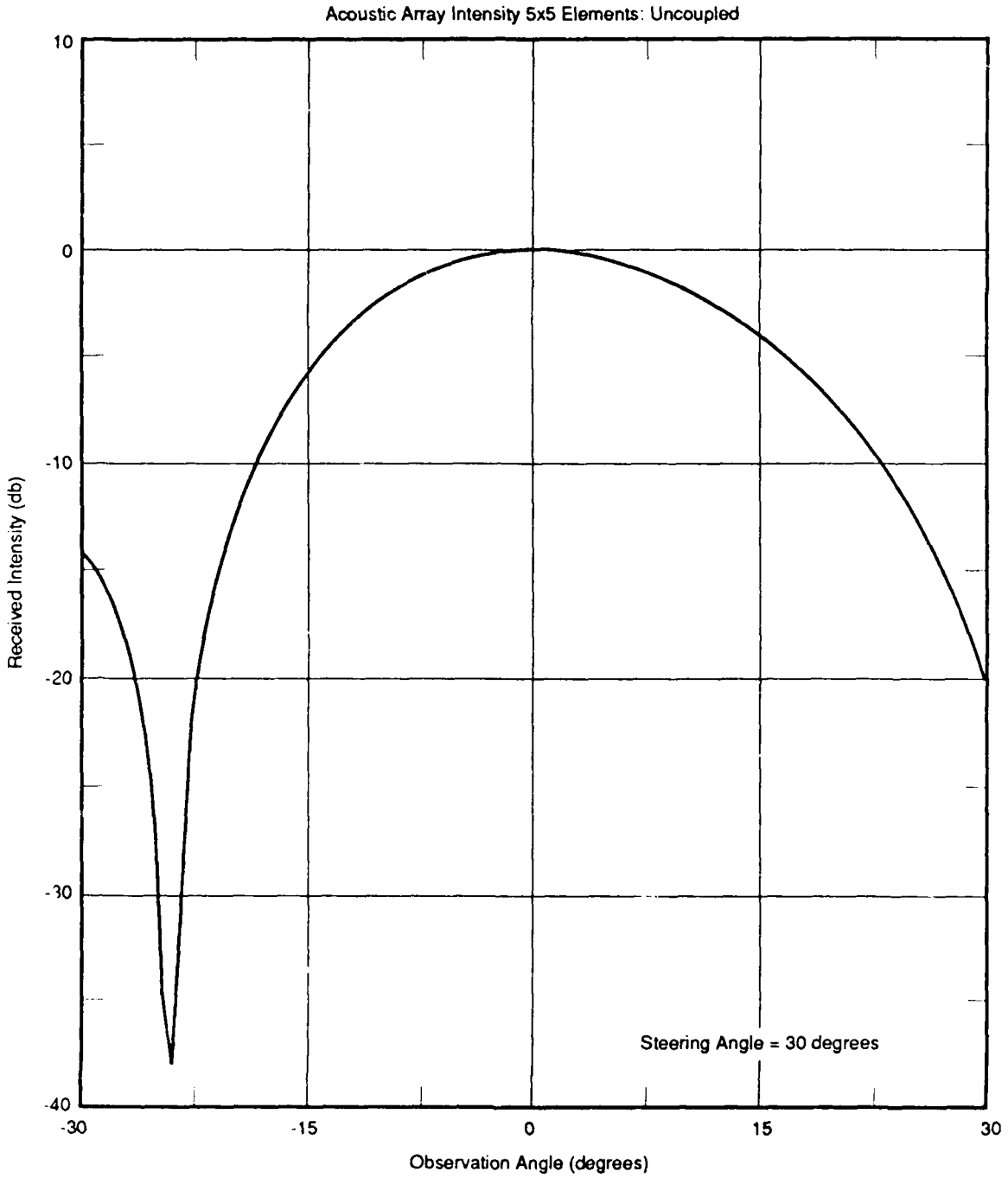

Figure 16 The radiated power, as in Figure (11), but for $\theta_s = 30°$.

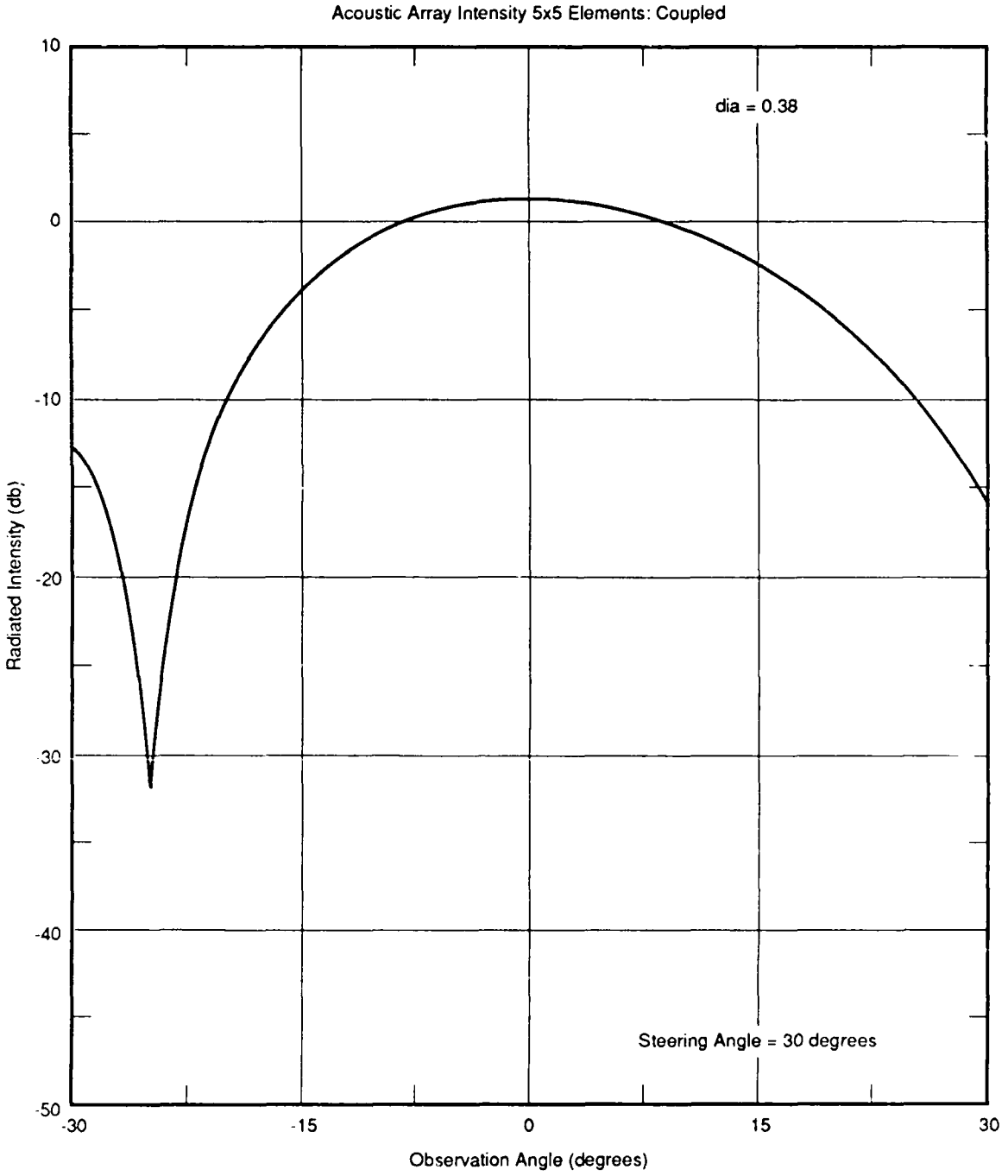

Figure 17 The radiated power, as in Figure (12), but for $\theta_S = 30^\circ$.

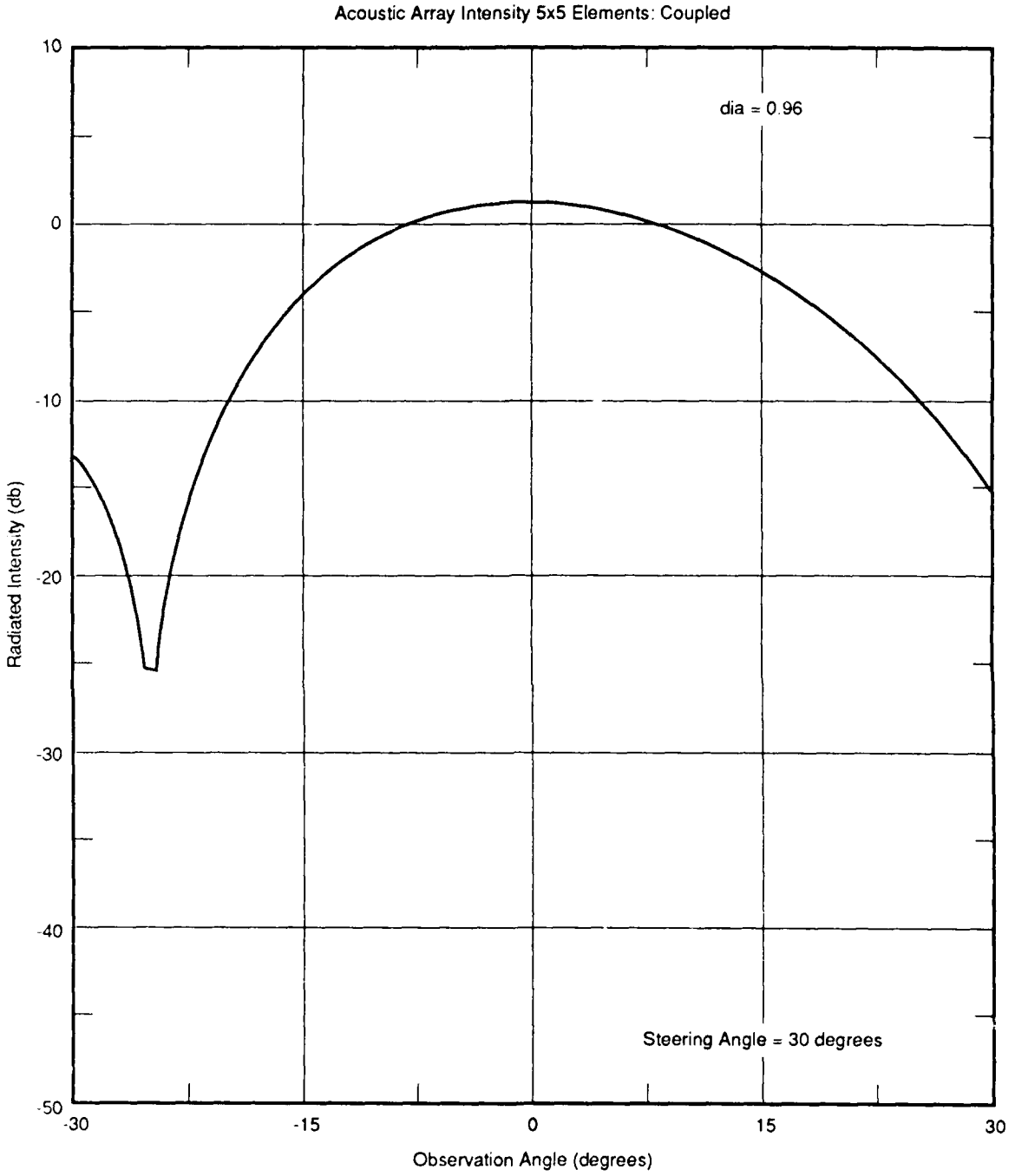

Figure 18 The radiated power, as in Figure (15), but for $\theta_S = 30°$.

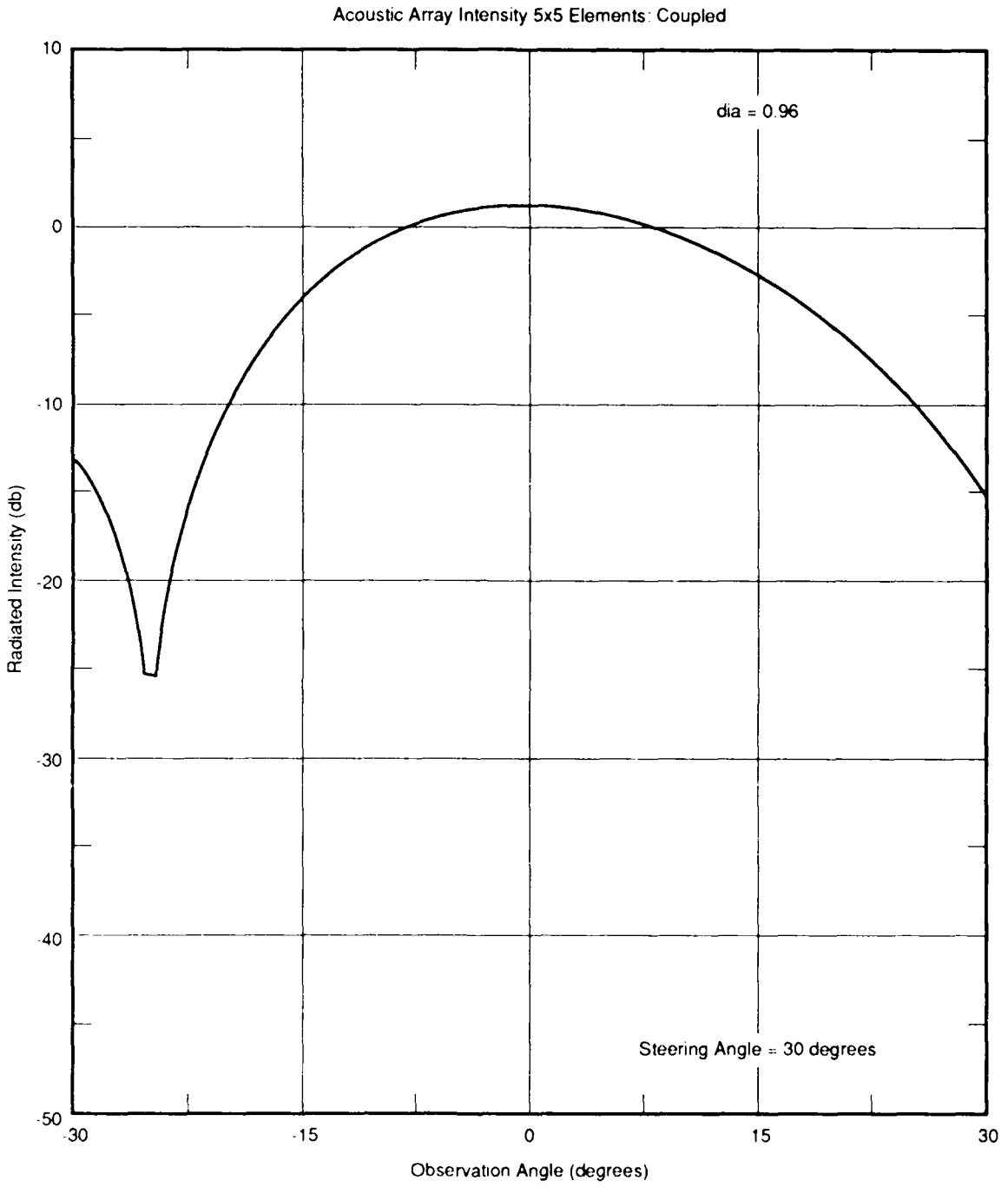

Figure 19 The largest element excitation (3.26), normalized to that for the uncoupled system, is shown as a function of element diameter.

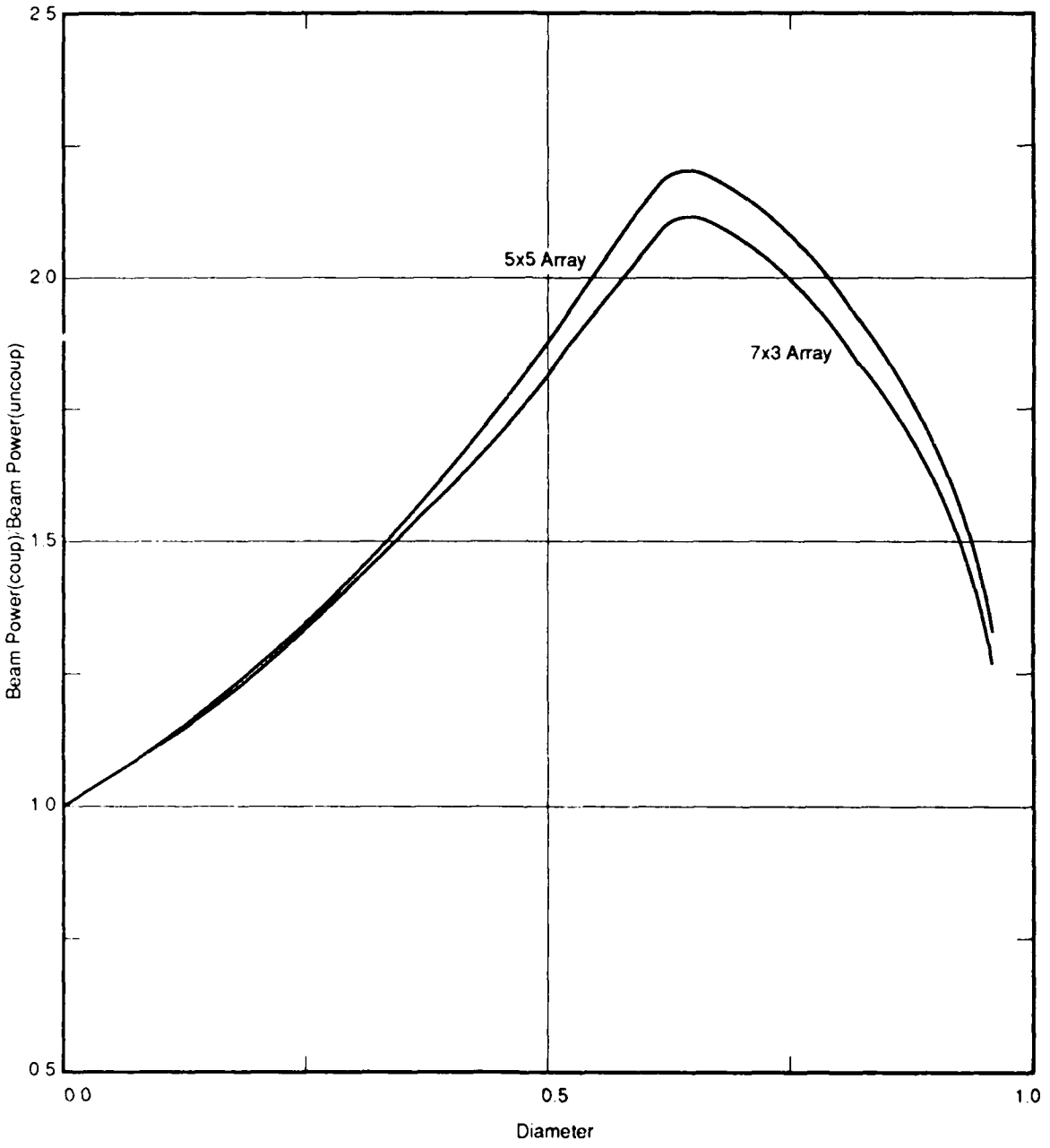

Figure 20 The beam power is shown as a function of element diameter.

increases the radiated power (holding fixed the driving forces). This is illustrated in Figure 19 where the largest element excitation

$$\frac{|V_i|^2 \max}{|V_0|^2} \qquad (3-26)$$

is shown as a function of the element diameter. The corresponding beam power is shown in Figure 20. Perhaps the most obvious effect of beam coupling is to reduce the minimum radiated power between beam lobes–a not surprising result, as this results from a delicate balance of phases.

For a linear array, the effects of element coupling can in principle be compensated for by adjusting the driving forces f_i. The practical consequences of coupling for beamforming do not seem to be very great, however.

DISTRIBUTION LIST

Director
DARPA
1400 Wilson Boulevard
Arlington, VA 22209-2308

Dr. Marvin C. Atkins [3]
Deputy Director
Science and Technology
Defense Nuclear Agency
6801 Telegraph Road
Alexandria, VA 22310

The Honorable John A. Betti
Undersecretary of Defense for Acquisition
The Pentagon, Room 3E933
Washington, DC 20301-3000

Dr. Arthur E. Bisson
Technical Director of Submarine
and SSBN Security Program
Department of the Navy, OP-02T
The Pentagon, Room 4D534
Washington, DC 20350-2000

Mr. Edward C. Brady
Sr. Vice President and General Manager
The MITRE Corporation
Mail Stop Z605
7525 Colshire Drive
McLean, VA 22102

The Honorable D. Allan Bromley
Asst to the President for Science and
Technology
Office of Science and Technology Policy
Old Executive Office Building, Room 360
17th & Pennsylvania Avenue, N.W.
Washington, DC 20506

Mr. Edward Brown
DARPA/PM
1400 Wilson Boulevard
Arlington, VA 22209-2308

Dr. Herbert L. Buchanan, III
Director
DARPA/DSO
1400 Wilson Boulevard
Arlington, VA 22209-2308

Dr. Ferdinand N. Cirillo, Jr.
Central Intelligence Agency
Washington, DC 20505

Mr. John Darrah
Senior Scientist and Technical Advisor
HQAF SPACOM/CN
Peterson AFB, CO 80914-5001

Dr. Russ E. Davis
Scripps Institution of Oceanography
A-030
University of California/San Diego
La Jolla, CA 92093

DTIC [2]
Defense Technical Information Center
Cameron Station
Alexandria, VA 22314

DISTRIBUTION LIST

Maj Gen Robert D. Eaglet
Assistant Deputy SAF/AQ
The Pentagon, Room 4E969
Washington, DC 20330-1000

Mr. John N. Entzminger
Director
DARPA/TTO
1400 Wilson Boulevard
Arlington, VA 22209-2308

Dr. Robert Foord [2]
Central Intelligence Agency
Washington, DC 20505

Dr. Larry Gershwin
Central Intelligence Agency
Washington, DC 20505

Dr. S. William Gouse
Sr. Vice President and General Manager
The MITRE Corporation
Mail Stop Z605
7525 Colshire Drive
McLean, VA 22102

LTGEN Robert D. Hammond
Commander and Program Executive Officer
U.S. Army / CSSD-ZA
Strategic Defense Command
P.O. Box 15280
Arlington, VA 22215-0150

Mr. Thomas H. Handel
Office of Naval Intelligence
The Pentagon
Room 5D662
Washington, DC 20350-2000

Dr. William Happer
Department of Physics
Princeton University
Box 708
Princeton, NJ 08544

MAJGEN Jerry C. Harrison
Commander
U.S. Army Laboratory Command
2800 Powder Mill Road
Adelphi, MD 20783-1145

Dr. Robert G. Henderson
Director
JASON Program Office
The MITRE Corporation
7525 Colshire Drive, Z561
McLean, VA 22102

Mr. James V. Hirsch
Central Intelligence Agency
Washington, DC 20505

JASON Library [5]
The MITRE Corporation
Mail Stop: W002
7525 Colshire Drive
McLean, VA 22102

DISTRIBUTION LIST

Dr. O'Dean P. Judd
Chief Scientist
Strategic Defense Initiative Organization
Room 1E1083
The Pentagon
Washington, DC 20301-7100

Mr. Robert Madden [2]
Department of Defense
National Security Agency
ATTN: R-9 (Mr. Madden)
Ft. George G. Meade, MD 20755-6000

Mr. Charles R. Mandelbaum
U.S. Department of Energy
Code ER-32
Mail Stop: G-236
Washington, DC 20545

Mr. Arthur F. Manfredi, Jr.
OSWR
Central Intelligence Agency
Washington, DC 20505

Lt Gen George L. Monahan, Jr.
Director/SDIO D
Strategic Defense Initiative Organization
(AF)
The Pentagon
Washington, DC 20301-7100

MGEN Thomas S. Moorman, Jr.
Director of Space and SDI Programs
Code SAF/AQS
The Pentagon
Washington, DC 20330-1000

Dr. Julian C. Nall
Institute for Defense Analyses
1801 North Beauregard Street
Alexandria, VA 22311

Dr. Robert L. Norwood [2]
Acting Director for Space
and Strategic Systems
Office of the Assistant Secretary of the Army
The Pentagon, Room 3E374
Washington, DC 20310-0103

Mr. Gordon Oehler
Central Intelligence Agency
Washington, DC 20505

Dr. Peter G. Pappas
Chief Scientist
U.S. Army Strategic Defense Command
P.O. Box 15280
Arlington, VA 22215-0280

Mr. Jay Parness
Central Intelligence Agency
Washington, DC 20505

MAJ Donald R. Ponikvar
Strategic Defense Command
Department of the Army
P.O. Box 15280
Arlington, VA 22215-0280

DISTRIBUTION LIST

Mr. John Rausch [2]
NAVOPINTCEN Detachment, Suitland
4301 Suitland Road
Washington, DC 20390

Records Resources
The MITRE Corporation
Mailstop: W115
7525 Colshire Drive
McLean, VA 22102

Dr. Victor H. Reis
Deputy Director
DARPA
1400 Wilson Boulevard
Arlington, VA 22209-2308

Dr. Fred E. Saalfeld
Director
Office of Naval Research
800 North Quincy Street
Arlington, VA 22217-5000

BGEN Anson Schulz
Acting Deputy Director
Strategic Defense Initiative Organization
1E1081
The Pentagon
Washington, DC 20301

Dr. Philip A. Selwyn [2]
Director
Office of Naval Technology
800 North Quincy Street Room 907
Arlington, VA 22217-5000

The Honorable Michael P.W. Stone
Secretary of the Army
Washington, DC 20310-0101

Superintendent
Code 1424
Attn: Documents Librarian
Naval Postgraduate School
Monterey, CA 93943

Dr. Vigdor Teplitz
ACDA/SPSA
320 21st Street, N.W.
Room 4923
Washington, DC 20451

Ms. Michelle Van Cleave
Assistant Director for National Security Affairs
Office of Science and Technology Policy
New Executive Office Building
17th and Pennsylvania Avenue
Washington, DC 20506

Mr. Richard Vitali
Director of Corporate Laboratory
U.S. Army Laboratory Command
2800 Powder Mill Road
Adelphi, MD 20783-1145

Dr. Kenneth M. Watson
Marine Physical Laboratory
Scripps Institution of Oceanography
University of California/Mail Code P-001
San Diego, CA 92152

DISTRIBUTION LIST

Mr. Robert Williams
Chief of Advanced Technology
DARPA
1400 Wilson Boulevard
Arlington, VA 22209-2308

RADM (Sel) Ray Witter
Director – Undersea Warfare
Space and Naval Warfare Systems Command
Code: PD-80
Department of the Navy
Washington, DC 20363-5100

ADM Daniel J. Wolkensdorfer
Director
DASWD (OASN/RD&A)
The Pentagon
Room 5C676
Washington, DC 20350-1000

Mr. Charles A. Zraket
President and Chief Executive Officer
The MITRE Corporation
Mail Stop A265
Burlington Road
Bedford, MA 01730